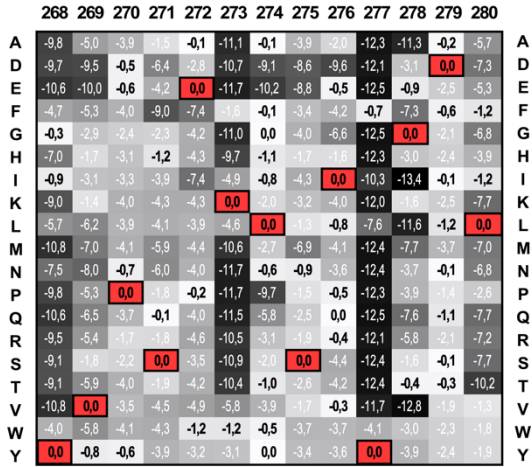


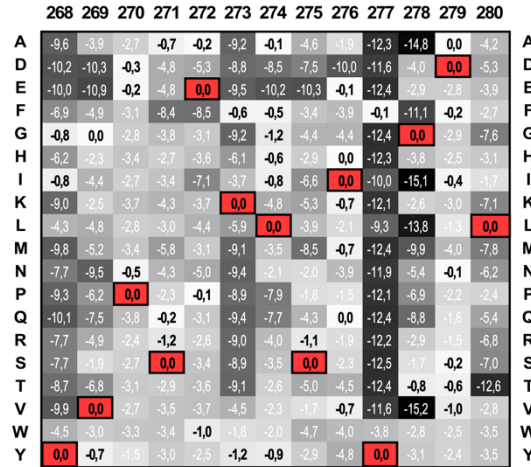
SUPPLEMENTARY FIGURES

a

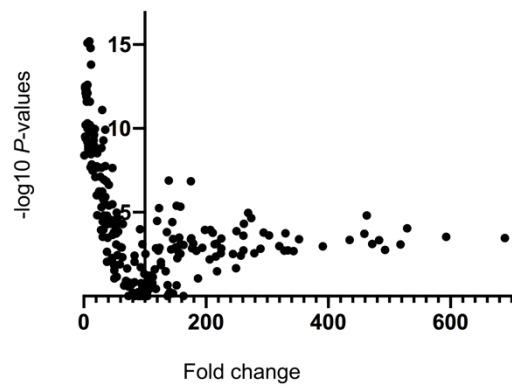
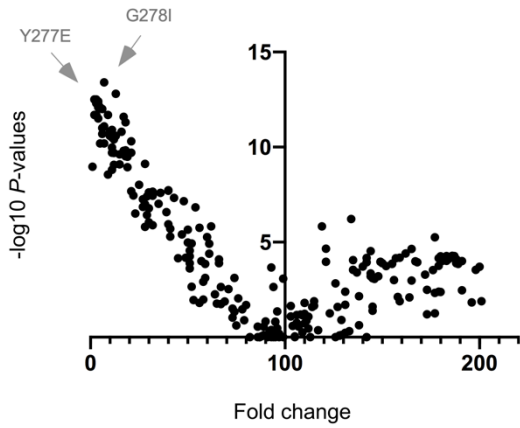
800, 600, 400 μM
(*P*-values; log₁₀)



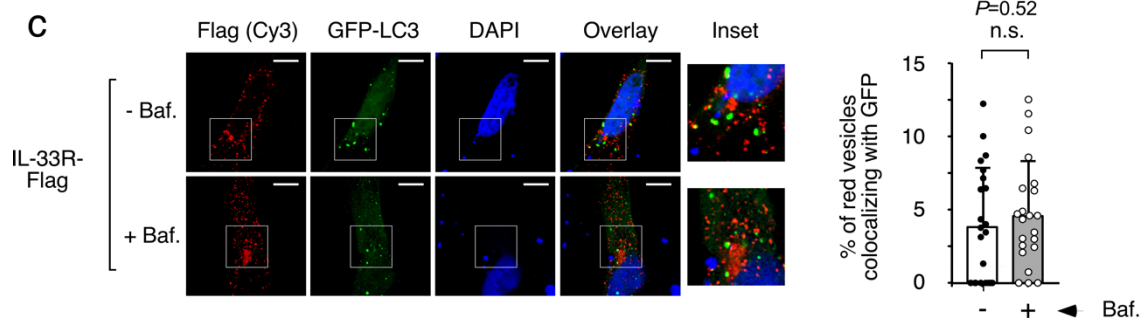
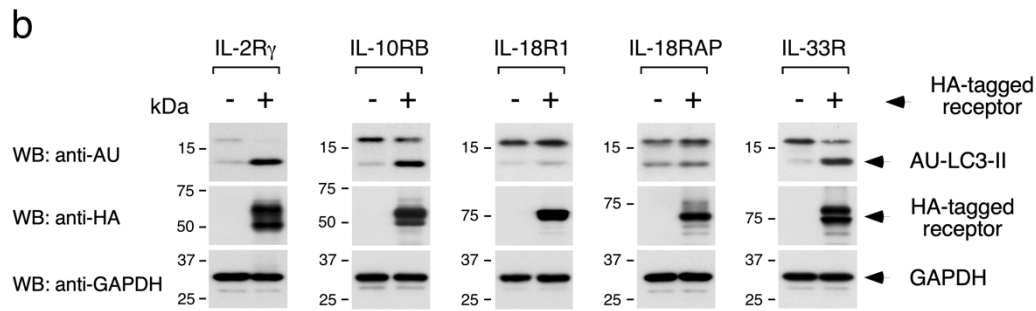
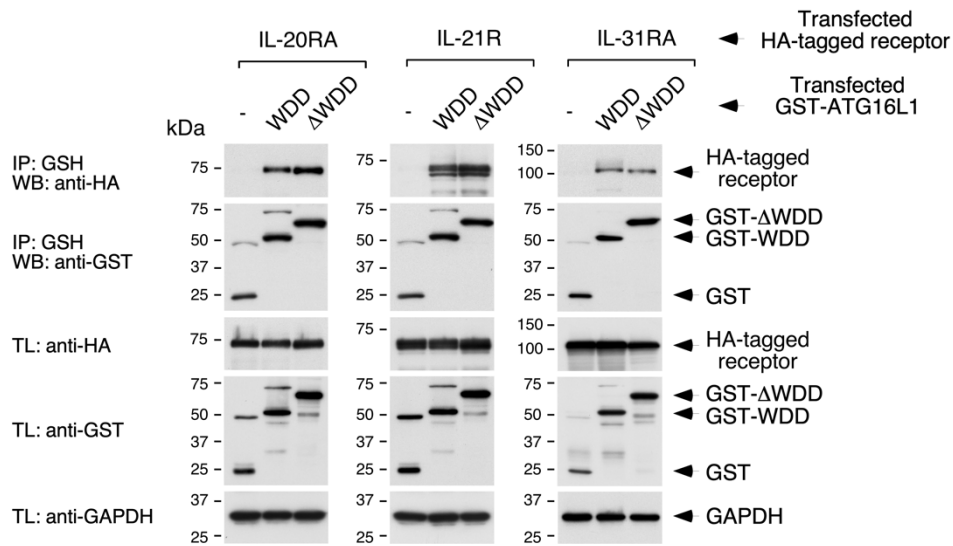
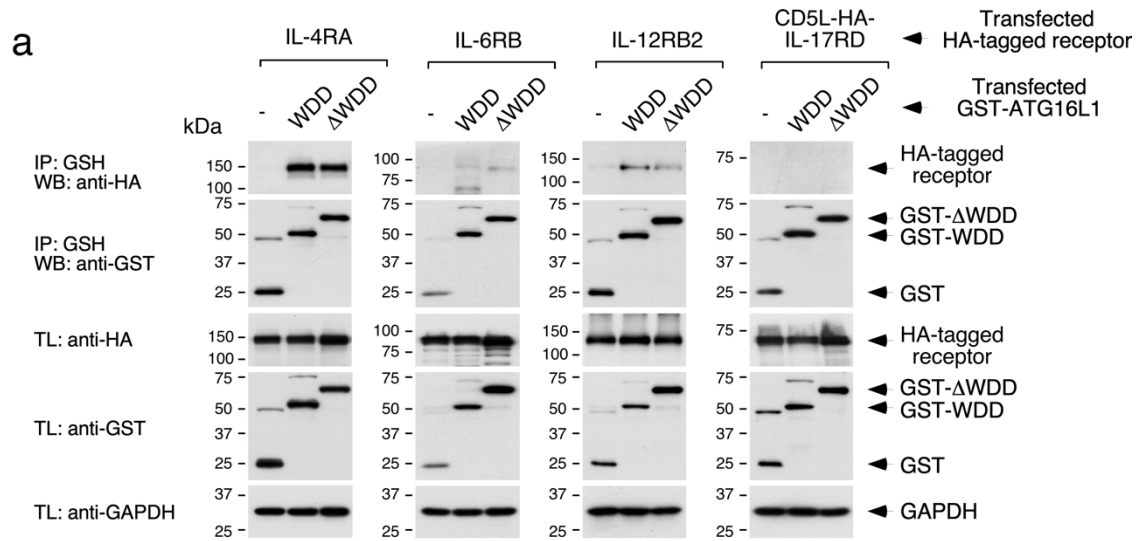
200, 50, 20 μM
(*P*-values; log₁₀)



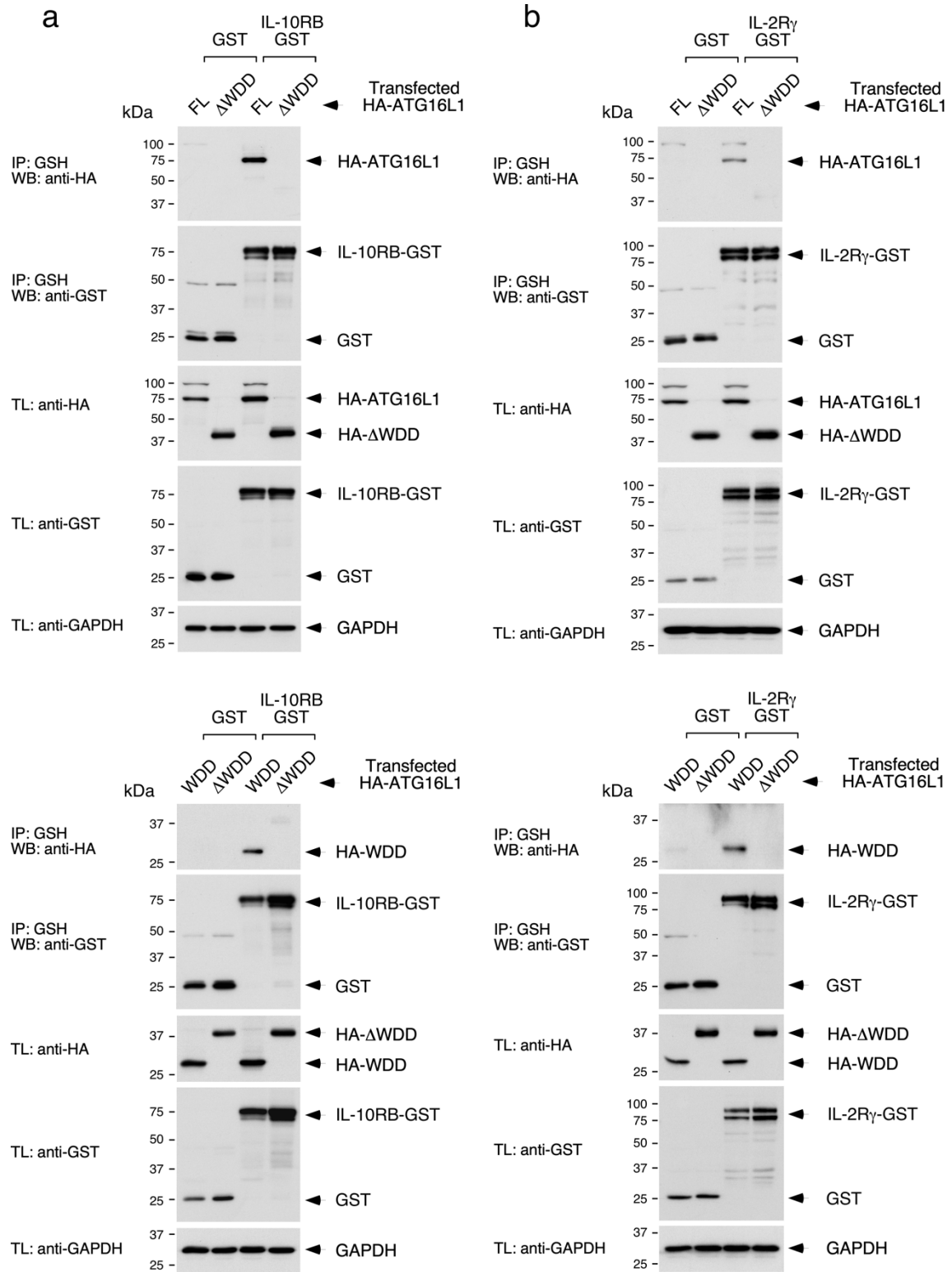
b



Supplementary Figure 1. Statistics of peptide microarray WDD binding studies. a, Heatmaps displaying \log_{10} P -values of the differences in binding activity observed between a given mutant and the wild-type peptide (n=8 experimental points). Numbers below -1,3 (P -value>0,05; significant differences) are shown in white font; values above this threshold are not significant and are represented in black/bold font. Squares are coloured following a continuous grey scale from low (white) to high (black) significance (lower P -value). Squares in red represent the native aminoacids present at each position in the 268-280 TMEM59 peptide. **b,** Volcano plots representing fold changes in the binding activity of the mutant peptides against the statistical significance of the change ($-\log_{10}$ P -values). Examples of 2 substitutions showing particularly strong binding defects that are highly significant (Y277E and G278I) are indicated. Source data are provided as a Source Data file.



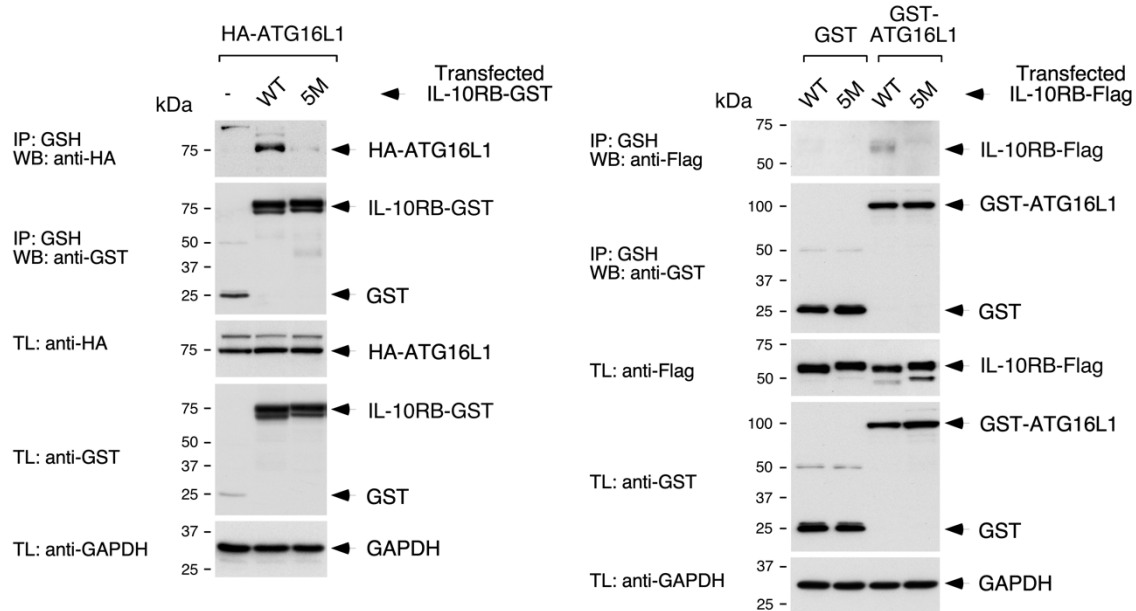
Supplementary Figure 2. Selection of candidate receptors. **a**, Co-immunoprecipitation studies to identify receptors able to specifically interact with the WDD. HEK-293T cells were co-transfected with tagged forms of the indicated cytokine receptors along with constructs including the WDD (320-607) or Δ WDD (1-319) fused to GST, as shown. Cells were lysed 36 h later and subjected to GST immunoprecipitation with agarose beads coupled to GSH. Shown are Western-blot against the indicated molecules. IP: immunoprecipitate; TL: total lysate. This panel shows candidate receptors unable to bind the WDD, or able to do so non-specifically due to additional interaction with Δ WDD. **b**, Evaluation of LC3 lipidation activity induced by the candidate cytokine receptors. HEK-293T cells were transfected with the indicated tagged cytokine receptors along with a plasmid expressing AU-LC3. Cells were lysed 36 h post-transfection for Western-blotting against the indicated molecules. **c**, Colocalization between transfected IL-33R and co-expressed GFP-LC3. HeLa cells were transfected with plasmids expressing IL-33R-Flag and GFP-LC3. Cells were treated for the last 6 h of culture with bafilomycin A1 (75 nM, as indicated), fixed 36 h post-transfection, stained with an anti-Flag antibody and scored for colocalization between the flag signal and GFP-LC3. Shown are representative confocal pictures (left), and a graph displaying the percentage of Flag-positive vesicles colocalizing with the GFP-positive signal \pm s.d. (right; n=22 cells; n.s: $P>0,05$, two-sided Student's *t*-test). Source data are provided as a Source Data file.



Supplementary Figure 3. Co-immunoprecipitation studies between IL-10RB/IL-2Rg fused to GST and full-length or deleted HA-ATG16L1 constructs. HEK-293T cells were co-transfected with the indicated receptors (**a**, IL-10RB; **b**, IL-2Rg) fused to GST and the shown HA-tagged ATG16L1 constructs (WDD: 320-607; deltaWDD: 1-319). Cells were lysed 36 h later and subjected to GST immunoprecipitation with agarose beads coupled to GSH. Shown are Western-blot images against the indicated molecules. IP: immunoprecipitate; TL: total lysate. Source data are provided as a Source Data file.

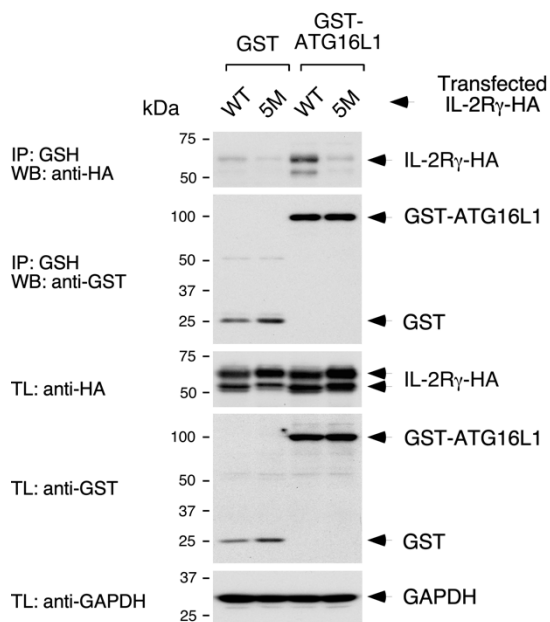
a

280 **FFsFplsdendvFdkL** 295 5M



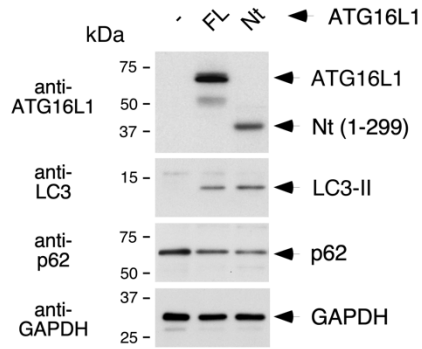
b

293 **lknLedLvteYhgnFsaW** 310 5M

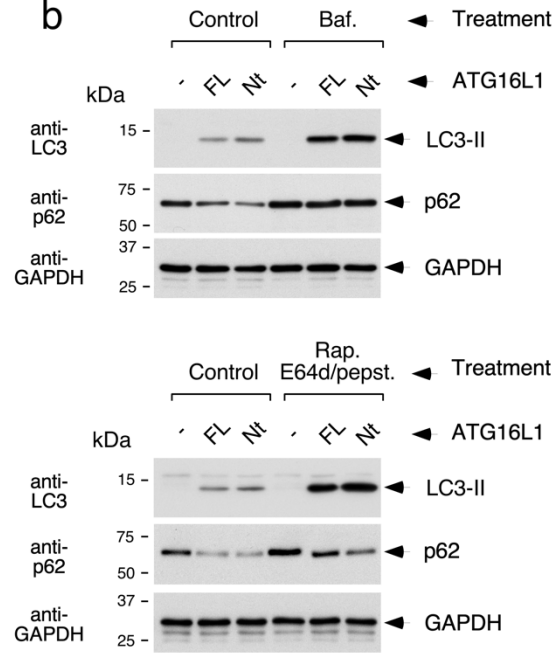


Supplementary Figure 4. Co-immunoprecipitation studies between wild-type or motif-mutated versions of IL-10RB/IL-2R_g and full-length ATG16L1. HEK-293T cells were co-transfected with wild-type (WT) or motif-mutated (5M, residues in red font mutated to alanine) forms of IL-10RB (**a**) or IL-2R_g (**b**) along with the indicated constructs expressing ATG16L1. Cells were lysed 36 h later and subjected to GST immunoprecipitation with agarose beads coupled to GSH. Shown are Western-blot images against the indicated molecules. IP: immunoprecipitate; TL: total lysate. Source data are provided as a Source Data file.

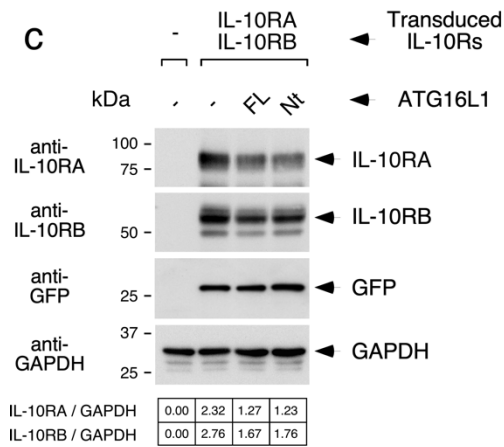
a



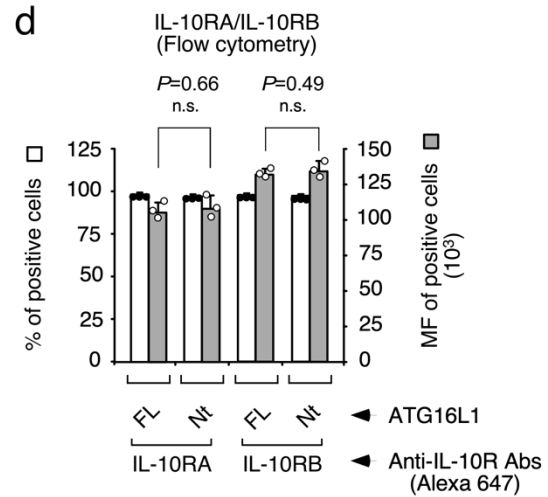
b



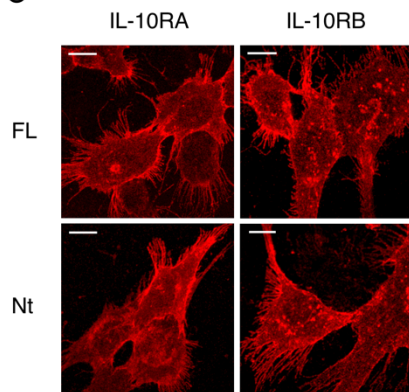
c



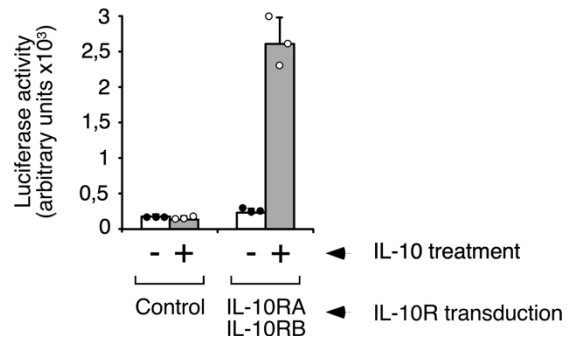
d



e

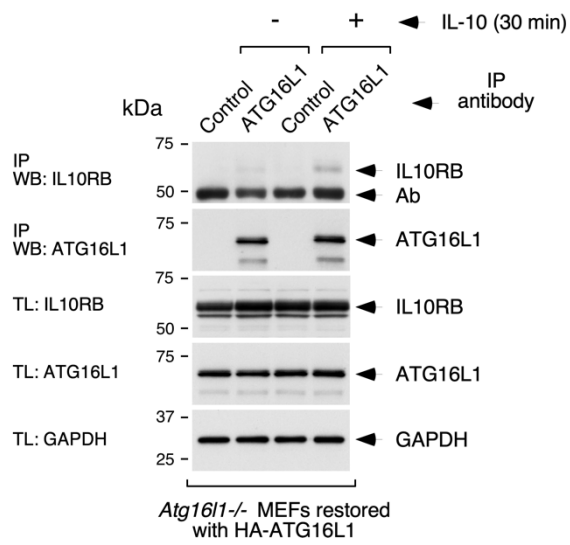


f

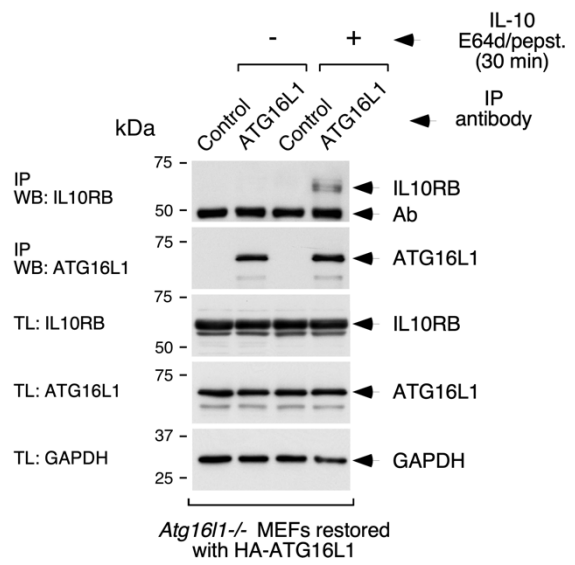


Supplementary Figure 5. Characterization of *Atg16L1*^{-/-} MEFs engineered to test the role of the WDD in IL-10 signalling. *Atg16L1*^{-/-} MEFs harbouring the STAT3-luciferase reporter and expressing STAT3 were restored with full-length ATG16L1 (FL) or a deleted version lacking the WDD (Nt, 1-299), and retrovirally transduced to express IL-10Rs A and B. **a**, Expression levels of full-length ATG16L1 (FL) and the N-terminal domain (1-299; Nt) in the engineered cells. The indicated cells were lysed for Western-blot against the shown molecules. **b**, Evaluation of autophagic flux in *Atg16L1*^{-/-} MEFs restored with FL or Nt. Cells were treated with bafilomycin A1 (75 nM, 6 h; top panel) or rapamycin (2 μ M) plus E64d/pepstatin (10 μ g/ml each; bottom panel) for 10 h, and lysed for Western-blotting with the shown antibodies. **c**, Expression levels of IL-10RA and IL-10RB in the engineered MEFs. Cells were lysed for Western-blot against the shown molecules. The anti-GFP blot detects GFP expression from an IRES-GFP cassette located downstream the IL-10RB open reading frame in the retroviral vector. Equal GFP expression levels argue that viral transduction was comparable in all cases, indicating that the increased IL-10R expression in *Atg16L1*^{-/-} cells is not due to enhanced transduction efficiency. Corrected densitometric quantifications are shown at the bottom of the Western-blot images. **d**, Surface expression levels of IL-10Rs. Cells were subjected to flow cytometry with specific anti-IL-10RA and -IL-10RB antibodies. Shown are the average percentage of positive cells with respect to control cells lacking IL-10Rs (left axis, white bars, solid dots) and the average mean of fluorescence of the positive cells (MF, right axis, grey bars, white dots), from triplicate experimental points \pm s.d. (n=3; n.s. *P*-value>0,05, two-sided Student's *t*-test)). A scheme of the gating and quantification strategy is provided in Supplementary Figure 17. **e**, Surface expression levels of IL-10Rs measured by immunofluorescence. The indicated unpermeabilized cells were stained *in vivo* with the same directly-conjugated anti-IL-10R antibodies as in **d** and fixed for immunofluorescence. Shown are representative confocal pictures. **f**, STAT3-luciferase response activated by IL-10 in *Atg16L1*^{-/-} MEFs restored with full-length ATG16L1 and lacking or expressing IL-10Rs. The indicated cells were treated with IL-10 (50 ng/ml; 8 h) and lysed to measure luciferase activity. Shown are mean values \pm s.d. of a representative experiment carried out in triplicate experimental points (n=3). Source data are provided as a Source Data file.

a

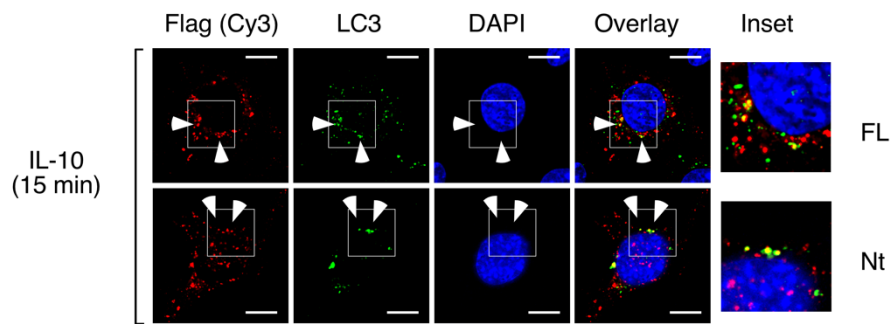
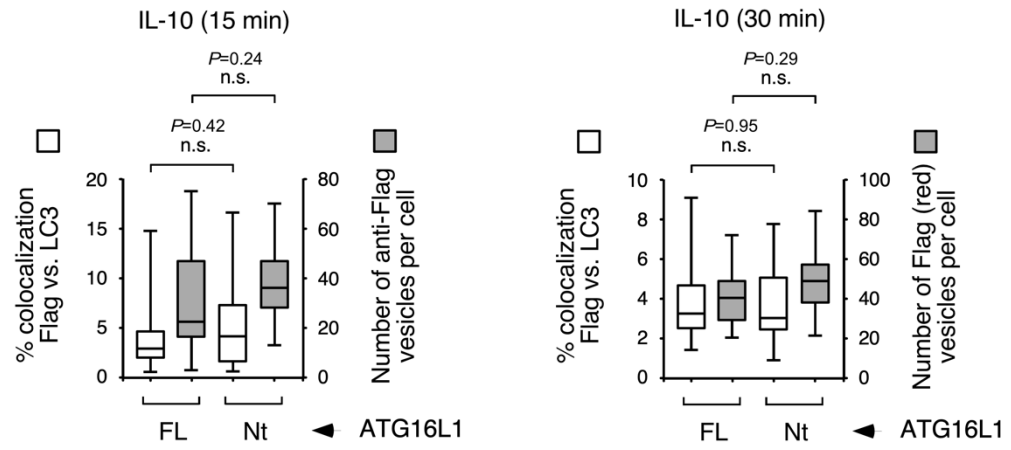


b

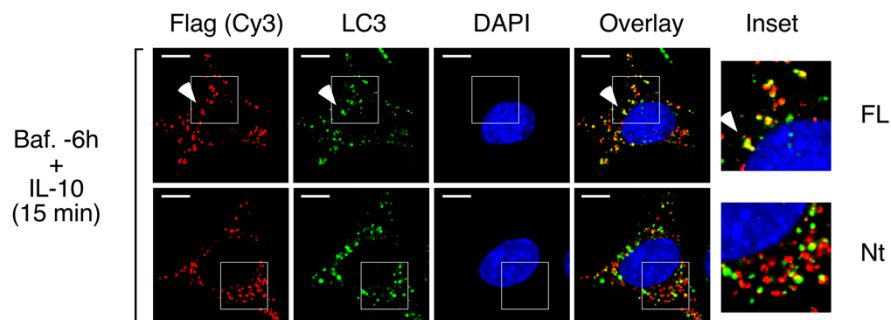
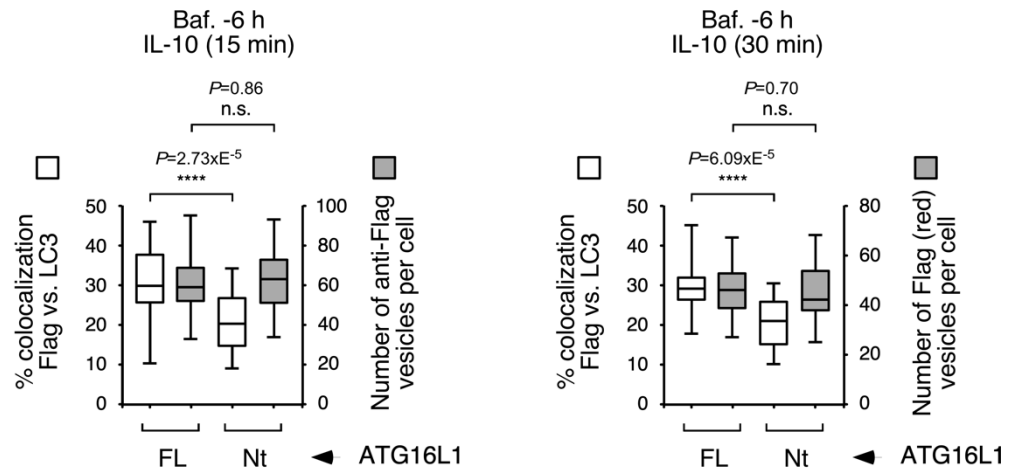


Supplementary Figure 6. IL-10-induced interaction between ATG16L1 and IL-10RB. *Atg16L1*^{-/-} MEFs restored with full-length ATG16L1, and engineered to express IL-10Rs (the same cell line characterized in Supplementary Fig. 5), were treated with IL-10 (50 ng/ml; 30 min; panel **a**) or with IL-10 (50 ng/ml) and E64d/pepstatin (10 ug/ml each) for 30 min (panel **b**). Cells were lysed for immunoprecipitation with control (irrelevant rabbit Ig) or anti-ATG16L1 antibodies (as displayed). Shown are Western-blot images against the indicated molecules. IP: immunoprecipitate; TL: total lysate. Ab refers to immunoprecipitating antibody signal. Source data are provided as a Source Data file.

a

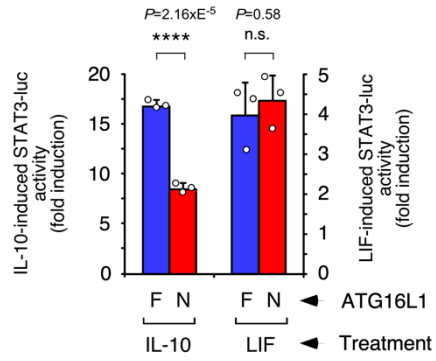


b

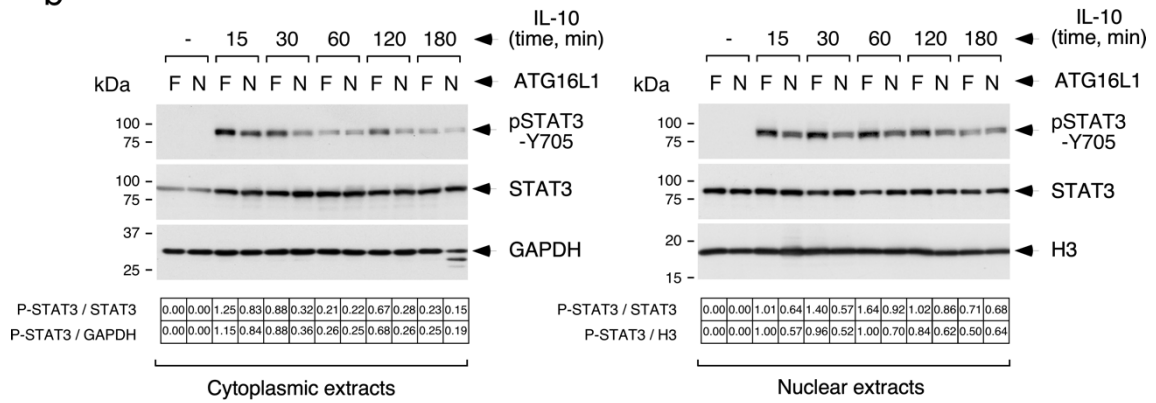


Supplementary Figure 7. Immunofluorescence assays to evaluate colocalization between IL-10RB and LC3 upon IL-10 treatment. The indicated engineered MEFs characterized in Supplementary Fig. 5 (FL: FL ATG16L1; N: Nt domain, 1-299), and expressing ectopic LC3 via retroviral transduction, were treated with IL-10 (50 ng/ml) for the shown times without **(a)** or with **(b)** a 6 h pre-incubation period with bafilomycin A1 (100 nM). Cells were then fixed for immunofluorescence with anti-Flag (IL-10RB, red) and anti-LC3 (green) antibodies. Shown are representative confocal pictures of the 15 min time points. Arrows indicate examples of colocalization events. Graphs show the percentage of colocalizing red (Flag) and green (LC3) signals per cell (left axis, white bars), and the total number of Flag-positive vesicles per cell (right axis, grey bars) under the different conditions. Data are presented as box-plots where the central line represents the median value, the box shows percentiles 25-75 and the whiskers include the most extreme values (n=20 cells except for colocalization in 15 min IL-10 where n=25, and -6 h Baf. + 15 min IL-10, where n=27 cells; n.s: $P > 0,05$; (***) : $P < 0.0001$, two-sided Student's *t*-test). Source data are provided as a Source Data file.

a

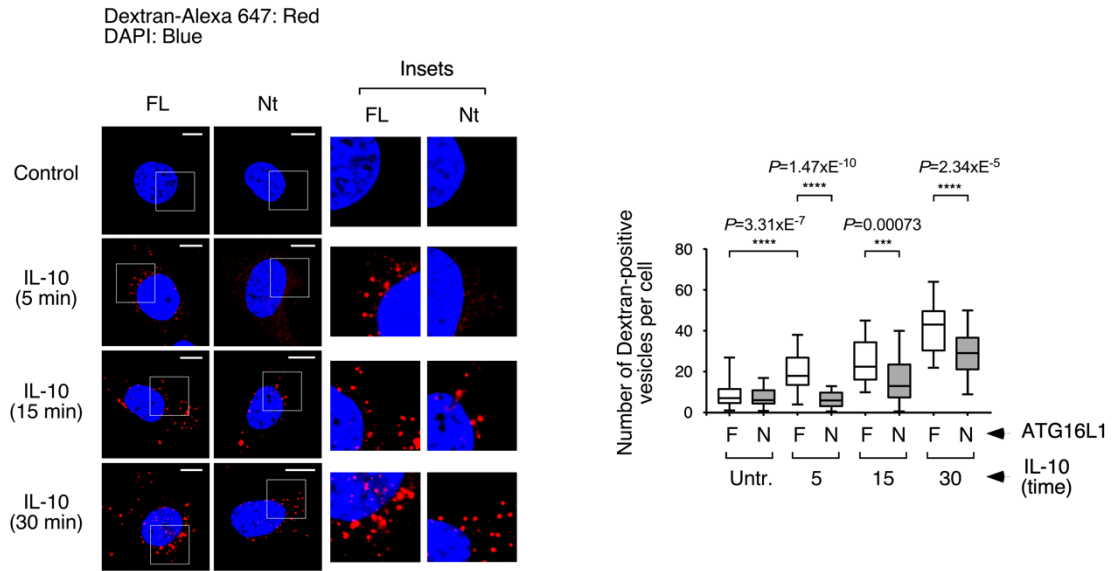


b

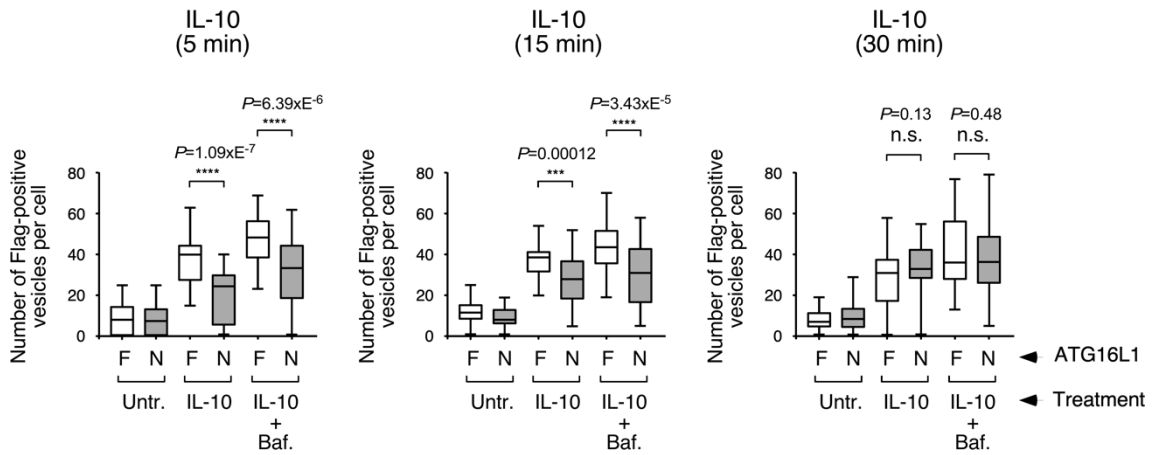


Supplementary Figure 8. a, Comparison of STAT3-luciferase activity induced by IL-10 and LIF in restored *Atg16L1*^{-/-} MEFs engineered to express IL-10Rs. The same cell lines characterized in Supplementary Fig. 5 (F: FL ATG16L1; N: Nt domain, 1-299) were treated with IL-10 (50 ng/ml; 4 h; left axis) or LIF (50 ng/ml; 2 h; right axis), and lysed to measure luciferase activity. Data are expressed as the mean of fold induction of luciferase activity \pm s.d obtained from triplicate experimental points (n=3; n.s.: $P>0.05$; (****): $P<0.0001$, two-sided Student's *t*-test) from a representative experiment. Blue bars: FL; Red bars: Nt. **b, IL-10-induced STAT3 phosphorylation.** Cells (F: FL ATG16L1; N: Nt domain) were continuously treated with IL-10 (50 ng/ml) for the shown times and lysed to obtain cytoplasmic and nuclear extracts for Western-blotting against the indicated molecules. Corrected densitometric quantifications are shown at the bottom of the Western-blot images. Source data are provided as a Source Data file.

a

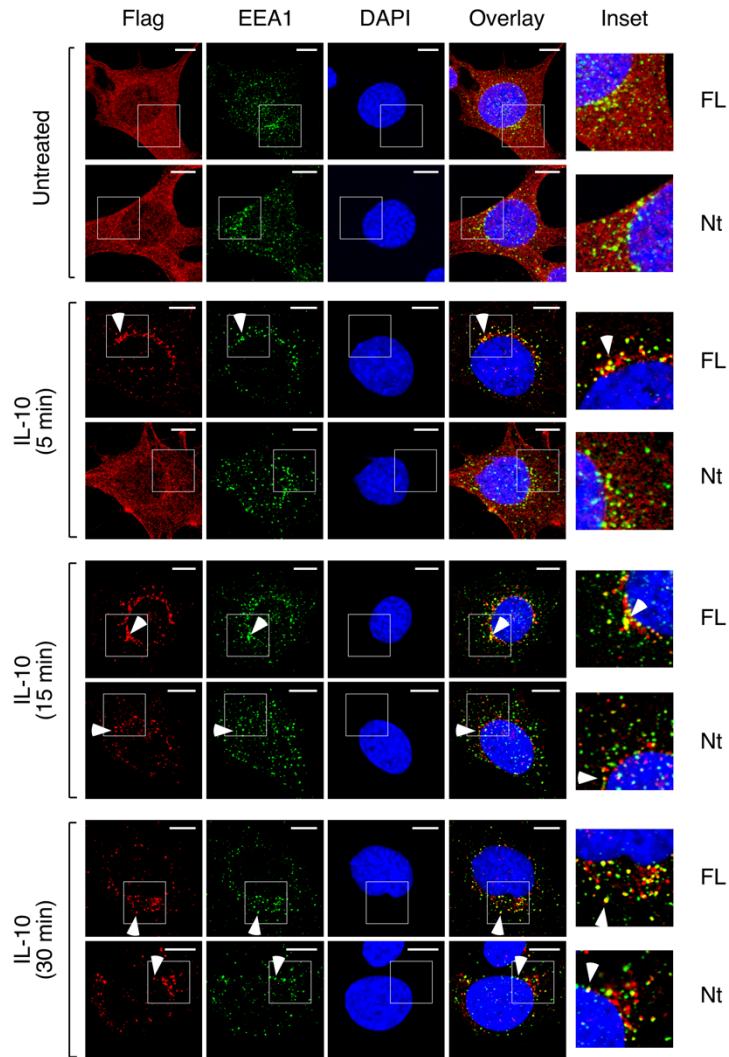


b

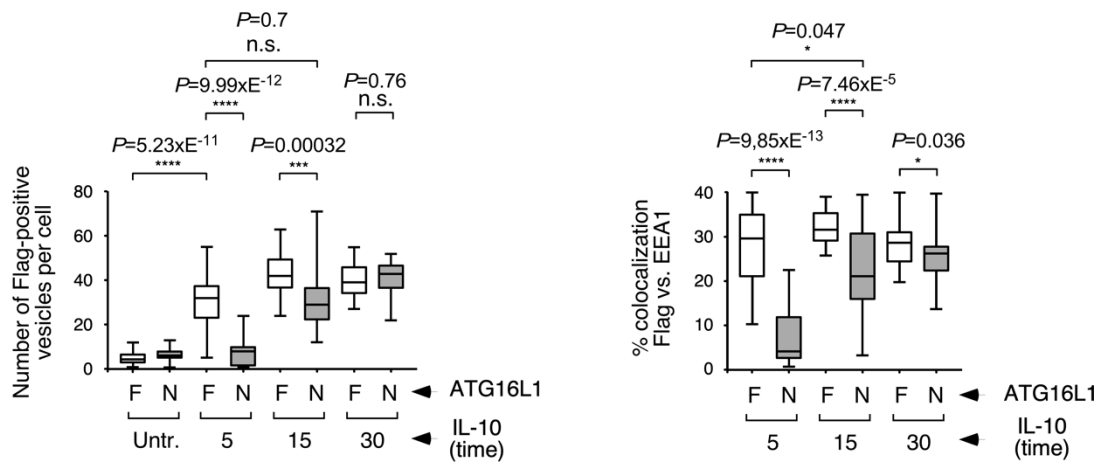


Supplementary Figure 9. a, Analysis of IL-10-induced endocytosis in cells expressing FL or Nt forms of ATG16L1 using dextran as an endocytic tracker. The indicated cells (FL or Nt) were co-incubated with IL-10 (50 ng/ml) and dextran-Alexa-647 (100 ug/ml) for the indicated times and then fixed and processed for immunofluorescence. Shown are representative confocal pictures (left). The numbers of dextran-positive vesicles per cell in the different conditions are presented as box-plots (right) where the central line represents the median value, the box shows percentiles 25-75 and the whiskers include the most extreme values (n=30 cells; (**): $P < 0.001$; (****): $P < 0.0001$, two-sided Student's *t*-test). **b, Pulse-chase experiment to evaluate the effect of bafilomycin in the number of intracellular IL-10RB-flag-positive vesicles induced by treatment with IL-10.** The indicated cell lines (FL or Nt) were pre-incubated with IL-10 (50 ng/ml; 30 min on ice) in the absence or presence of bafilomycin (75 nM, as indicated), washed to remove IL-10 and then chased for the indicated times (in the absence or presence of bafilomycin, as required) before fixation and staining for anti-Flag immunofluorescence. Box-plots display the number of Flag-positive vesicles per cell in the different conditions (the central line represents the median value, the box shows percentiles 25-75 and the whiskers include the most extreme values; n=40 cells except for untreated samples where n=20; n.s.: $P > 0.05$; (**): $P < 0.001$; (****): $P < 0.0001$, two-sided Student's *t*-test). Source data are provided as a Source Data file.

a

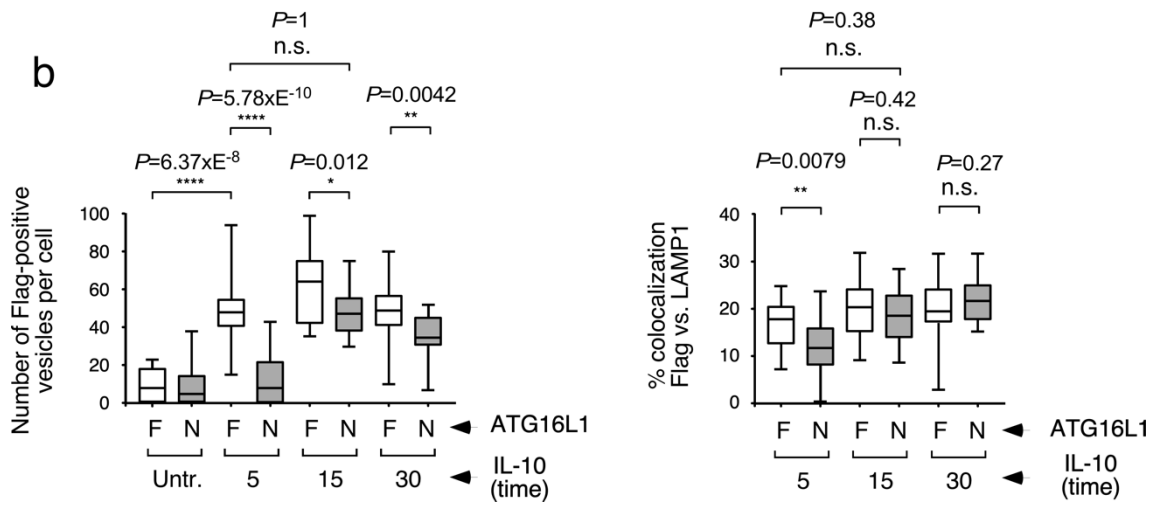
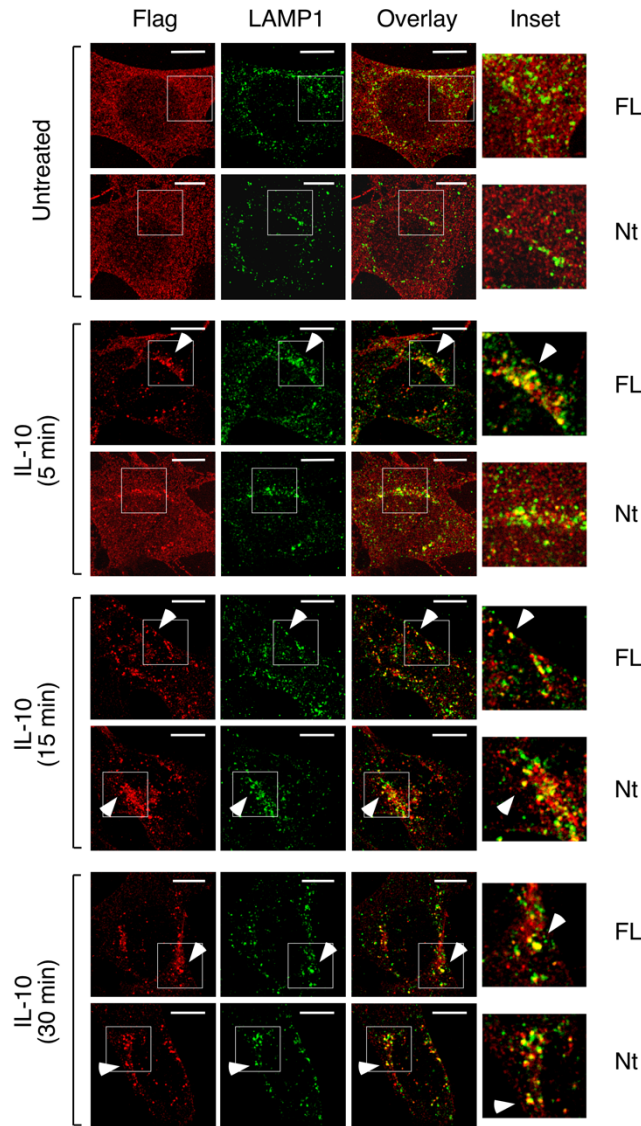


b



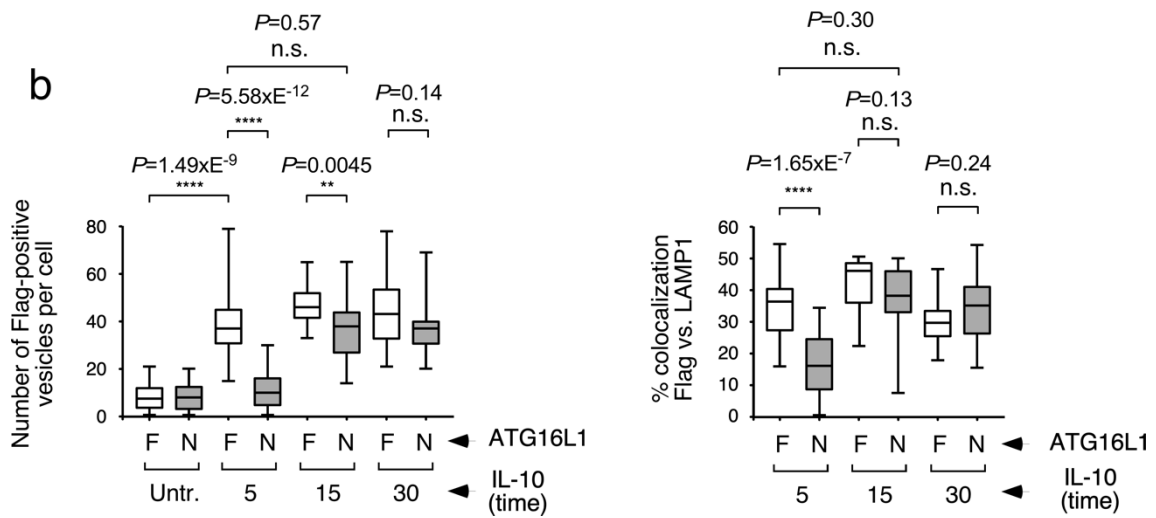
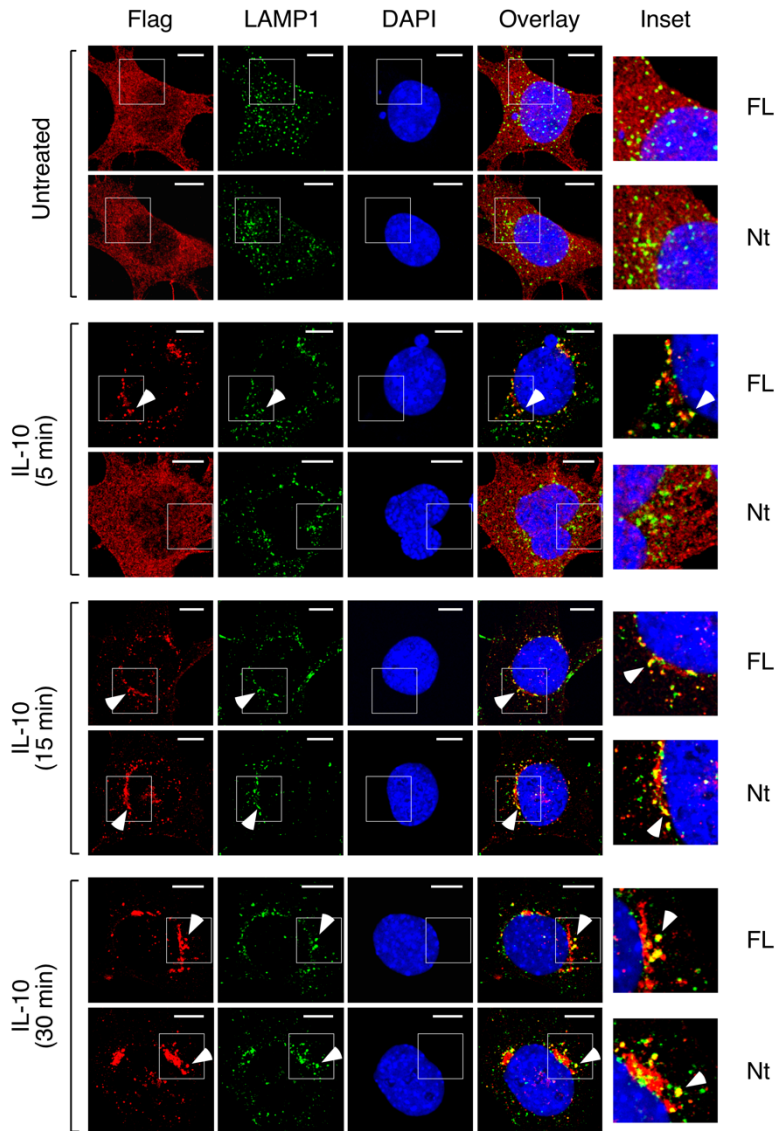
Supplementary Figure 10. Immunofluorescence pulse-chase assay to explore IL-10-induced IL-10RB endocytosis and intracellular trafficking to EEA1-positive compartments. **a**, The indicated cells (FL or Nt) were pre-incubated with IL-10 (50 ng/ml; 30 min on ice), washed to remove IL-10 and then chased for the indicated times before fixation and staining with anti-Flag (IL-10RB, red) and anti-EEA1 (green) antibodies. Shown are representative confocal pictures. Arrows indicate examples of colocalization events. **b**, Box-plots displaying quantification of the phenotypes observed in **a**. The left panel shows the number of Flag-positive vesicles per cell at different times after IL-10 treatment observed in this experiment. The right panel represents the percentage of colocalizing red (Flag) and green (EEA1) signals per cell. Data are presented as box-plots where the central line represents the median value, the box shows percentiles 25-75 and the whiskers include the most extreme values. For both panels, n=25 cells except for untreated cells (n=15); (n.s: $P > 0,05$; (*): $P < 0.05$; (**): $P < 0.001$; (****): $P < 0.0001$, two-sided Student's *t*-test). Source data are provided as a Source Data file.

a



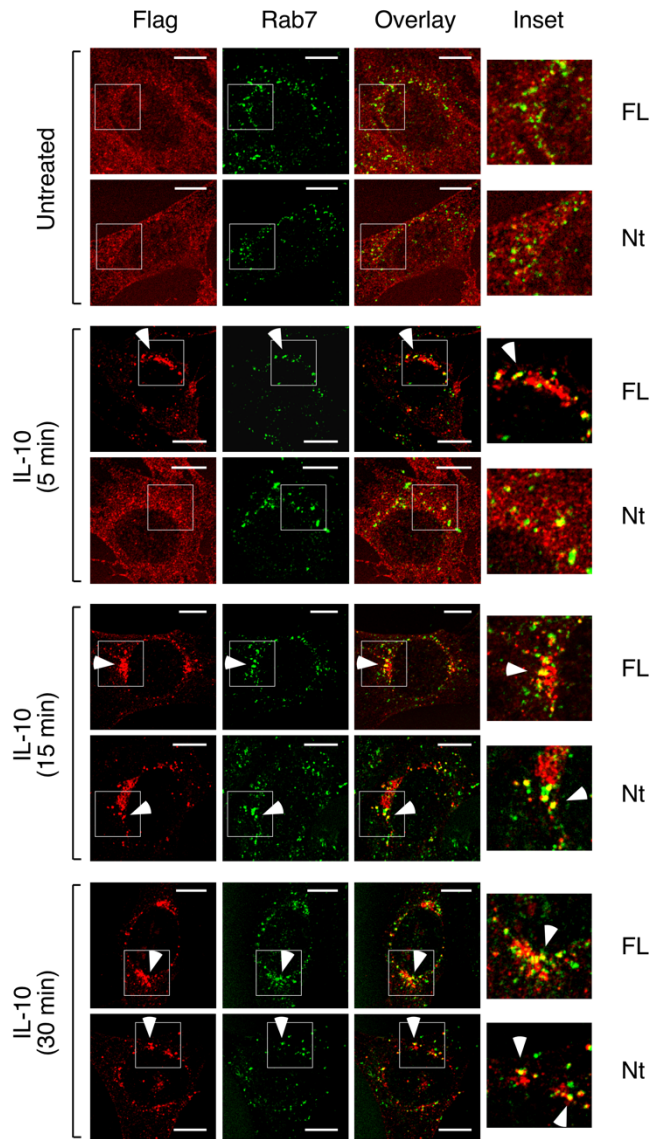
Supplementary Figure 11. Immunofluorescence assay to explore IL-10-induced IL-10RB endocytosis and intracellular trafficking to LAMP1-positive compartments. **a**, The indicated cells (FL or Nt) were continuously treated with IL-10 (50 ng/ml) for the shown times and fixed for immunofluorescence with anti-Flag (IL-10RB, red) and anti-LAMP1 (green) antibodies. Shown are representative confocal pictures. Arrows indicate examples of colocalization events. **b**, Box-plots displaying quantification of the phenotypes observed in **a**. The left panel shows the number of Flag-positive vesicles per cell at different times after IL-10 treatment observed in this experiment. The right panel represents the percentage of colocalizing red (Flag) and green (LAMP1) signals per cell. Data are presented as box-plots where the central line represents the median value, the box shows percentiles 25-75 and the whiskers include the most extreme values. For both panels, n=20 cells except for untreated cells (n=10); (n.s.: $P>0,05$; (*): $P<0.05$; (**): $P<0.01$; (****): $P<0.0001$, two-sided Student's *t*-test). Source data are provided as a Source Data file.

a

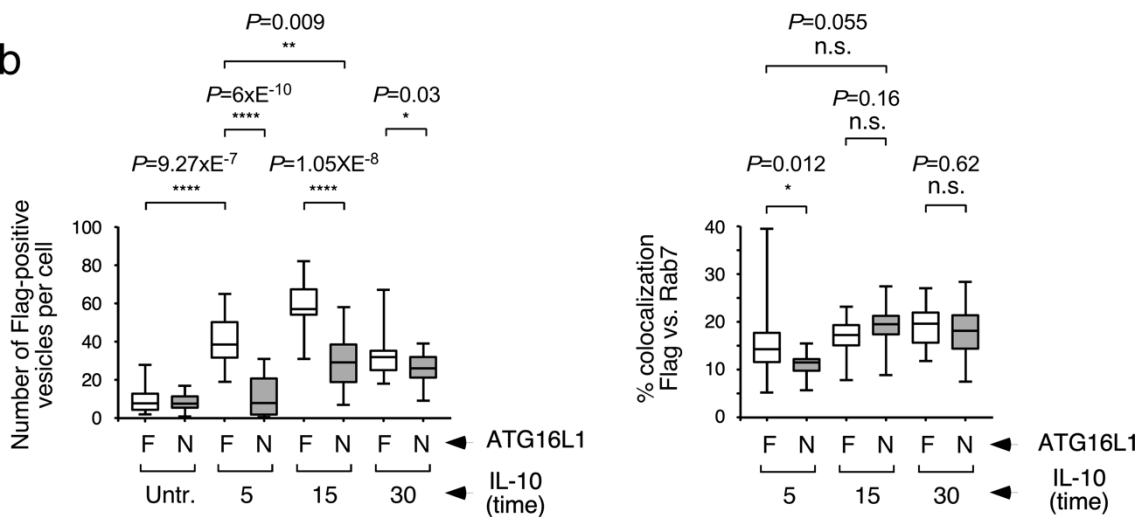


Supplementary Figure 12. Immunofluorescence pulse-chase assay to explore IL-10-induced IL-10RB endocytosis and intracellular trafficking to LAMP1-positive compartments. **a**, The indicated cells (FL or Nt) were pre-incubated with IL-10 (50 ng/ml; 30 min on ice), washed to remove IL-10 and then chased for the indicated times before fixation and staining with anti-Flag (IL-10RB, red) and anti-LAMP1 (green) antibodies. Shown are representative confocal pictures. Arrows indicate examples of colocalization events. **b**, Box-plots displaying quantification of the phenotypes observed in **a**. The left panel shows the number of Flag-positive vesicles per cell at different times after IL-10 treatment observed in this experiment. The right panel represents the percentage of colocalizing red (Flag) and green (LAMP1) signals per cell. Data are presented as box-plots where the central line represents the median value, the box shows percentiles 25-75 and the whiskers include the most extreme values. For both panels, n=25 cells except for untreated cells (n=14) (n.s: $P>0,05$; (**): $P<0.01$; (****): $P<0.0001$, two-sided Student's *t*-test). Source data are provided as a Source Data file.

a

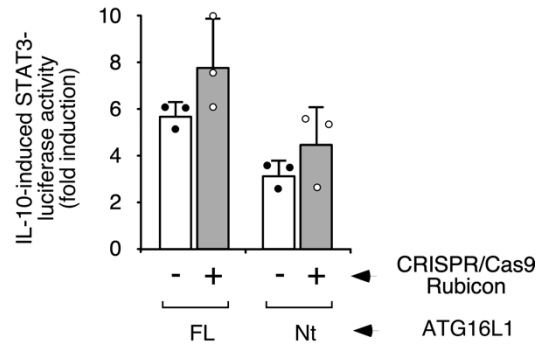
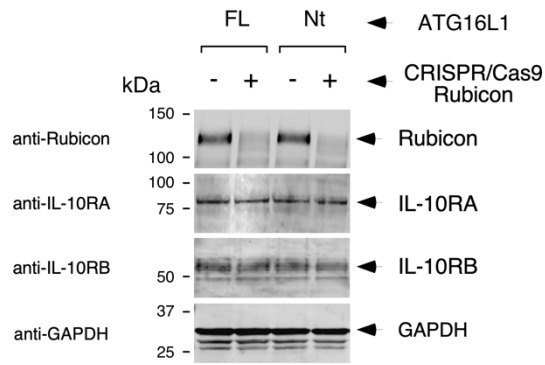


b

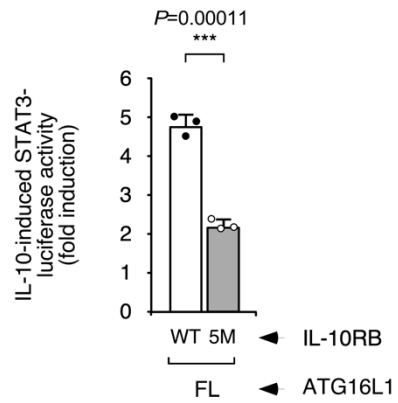
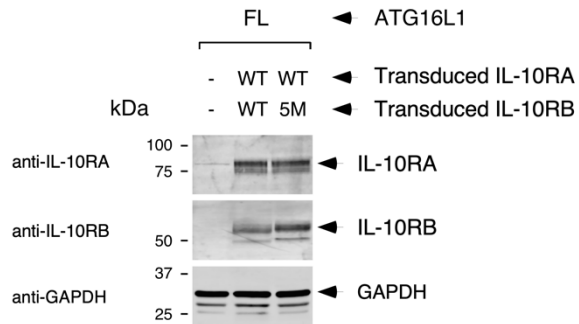


Supplementary Figure 13. Immunofluorescence assay to explore IL-10-induced IL-10RB endocytosis and intracellular trafficking to Rab7-positive compartments. **a**, The indicated cells (FL or Nt) were continuously treated with IL-10 (50 ng/ml) for the shown times and fixed for immunofluorescence with anti-Flag (IL-10RB, red) and anti-Rab7 (green) antibodies. Shown are representative confocal pictures. Arrows indicate examples of colocalization events. **b**, Box-plots displaying quantification of the phenotypes observed in **a**. The left panel shows the number of Flag-positive vesicles per cell at different times after IL-10 treatment observed in this experiment. The right panel represents the percentage of colocalizing red (Flag) and green (Rab7) signals per cell. Data are presented as box-plots where the central line represents the median value, the box shows percentiles 25-75 and the whiskers include the most extreme values. For both panels, n=20 cells except for untreated cells (n=14); n.s: $P > 0,05$; (*): $P < 0,05$; (**): $P < 0,01$; (****): $P < 0,0001$, two-sided Student's *t*-test. Source data are provided as a Source Data file.

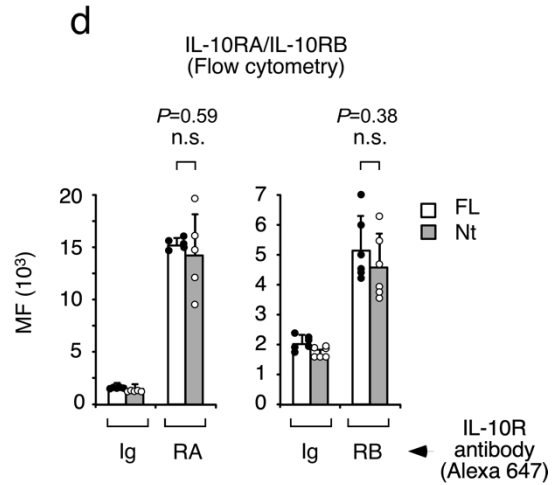
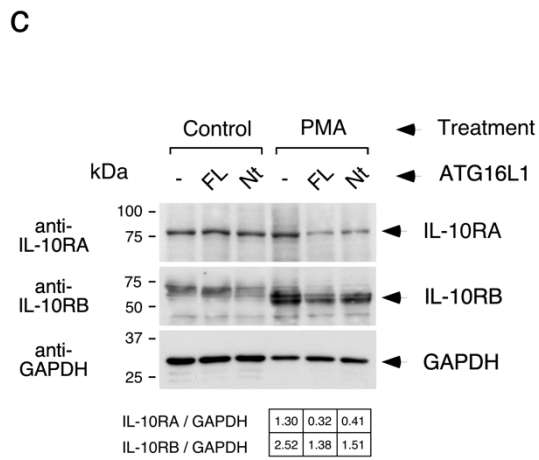
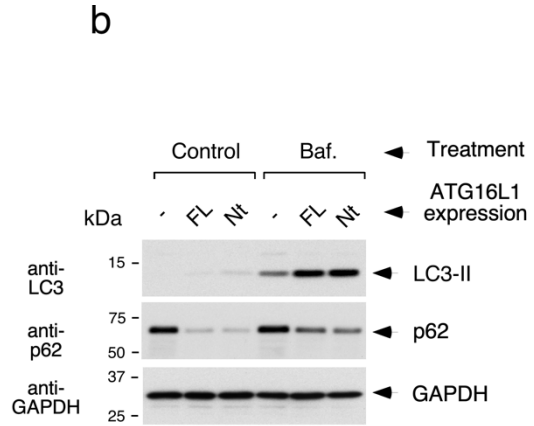
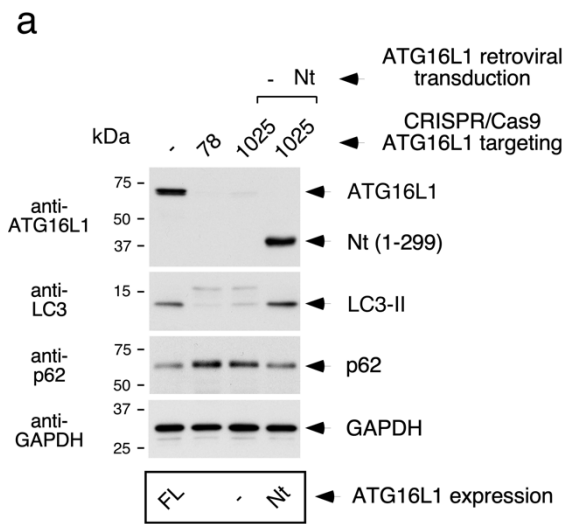
a



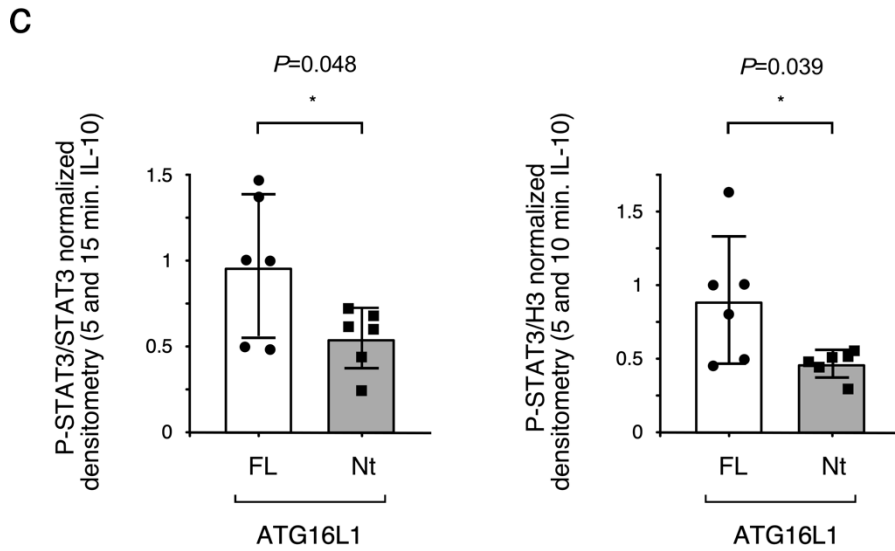
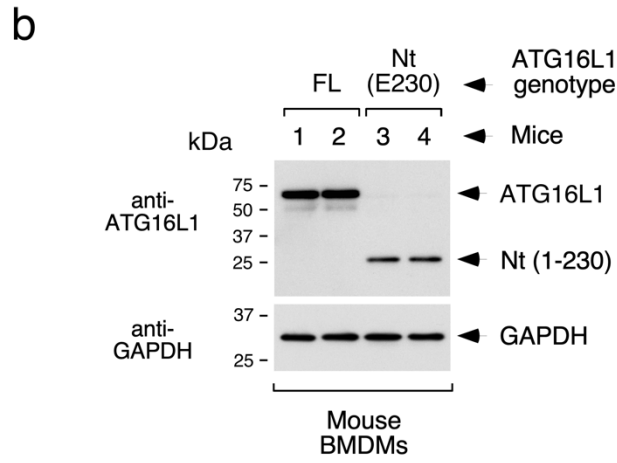
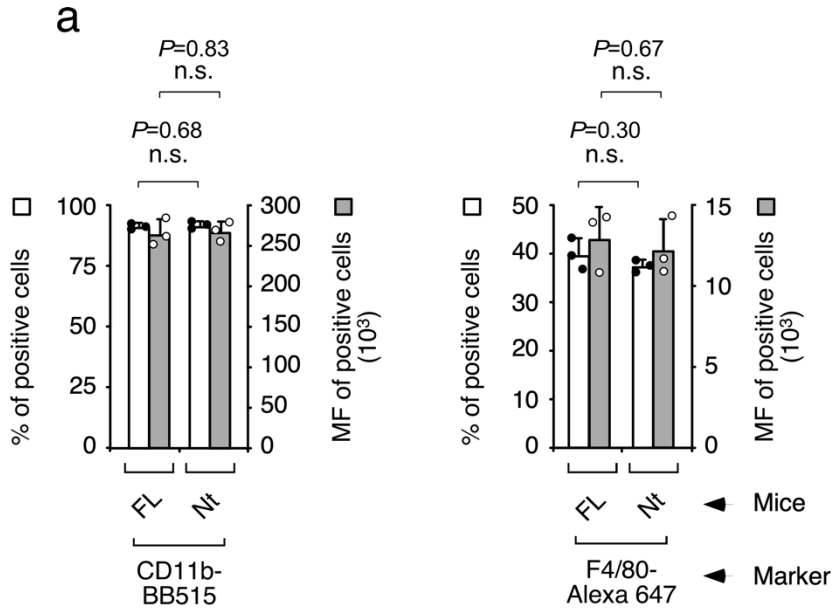
b



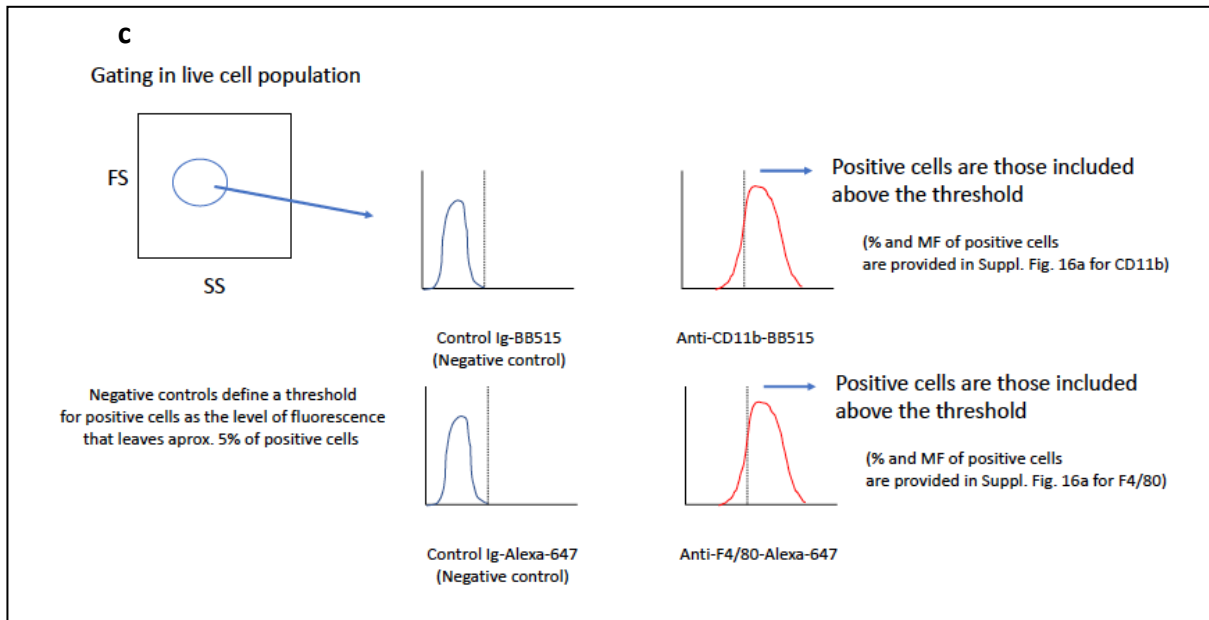
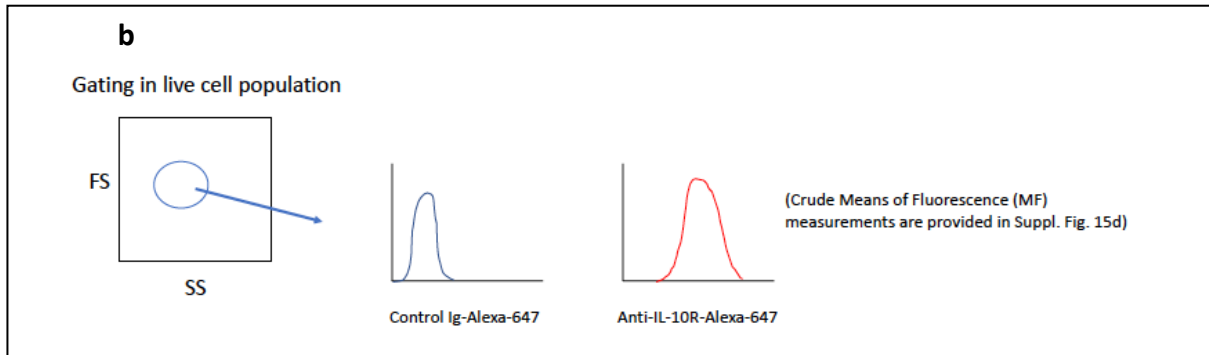
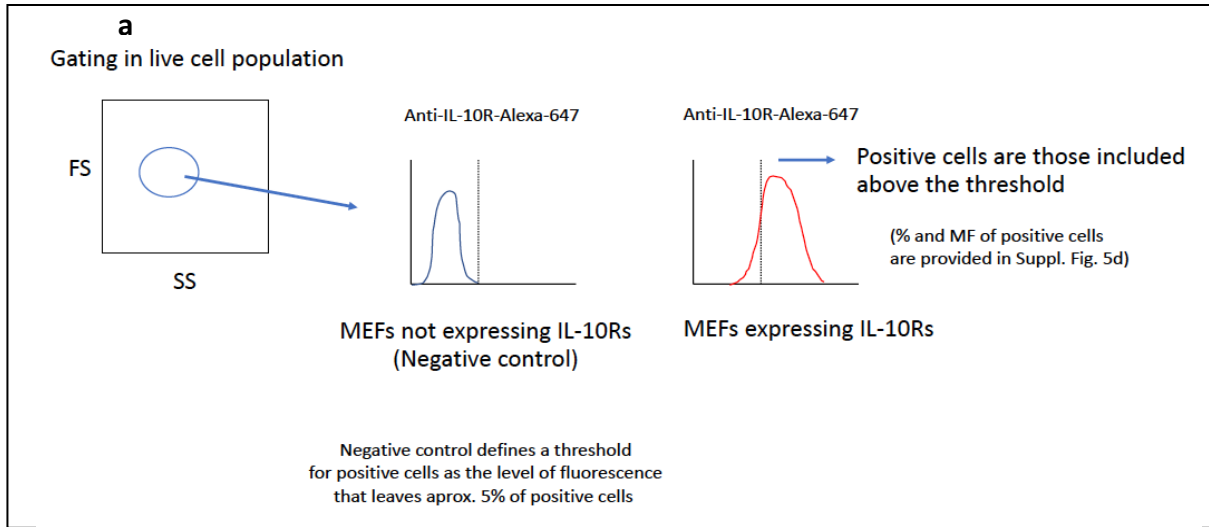
Supplementary Figure 14. a, Analysis of IL-10 signalling in FL and Nt cells depleted of Rubicon. FL- and Nt-expressing MEFs (as indicated) were transduced with lentiviral control (-) or Rubicon-specific (+) CRISPR/Cas9 constructs, selected in blasticidin (2 ug/ml) for 6 days, lysed to evaluate the expression of the indicated molecules by Western-blotting (left panel) and tested for IL-10-induced STAT3-luciferase activity (50 ng/ml, 4 h; right panel). Data are expressed as means of fold induction of luciferase activity \pm s.d. of 3 independent experiments each including triplicate experimental points (n=3). **b, Analysis of IL-10 signalling in cells expressing mutated IL-10RB (5M).** MEFs harbouring STAT3, the STAT3-luciferase reporter and FL ATG16L1 were transduced with retroviral constructs expressing IL-10RA and IL-10RB (WT or mutated (5M), as indicated), lysed 3 days later for Western-blotting against the indicated molecules (left panel) and tested for IL-10-induced STAT3-luciferase activity (50 ng/ml, 4 h; right panel). Data are expressed as means of fold induction of luciferase activity \pm s.d. of triplicate experimental points (***) $P < 0.001$, two-sided Student's *t*-test. Source data are provided as a Source Data file.



Supplementary Figure 15. Characterization of THP1 cells engineered to test the role of the WDD in IL-10 signalling through endogenous IL-10Rs. **a**, CRISPR/Cas9-induced depletion of endogenous ATG16L1 and restoration with a retroviral construct expressing the Nt domain (aminoacids 1-299). THP1 cells were transduced with lentiviral CRISPR/Cas9 constructs harbouring the indicated RNA guides directed to endogenous ATG16L1 (78: sgRNA recognizes positions 78-97 from the first coding nucleotide in ATG16L1 mRNA; 1025: sgRNA recognizes positions 1025-1044; (-): empty vector). Cells targeted with the 1025 guide were restored with a retroviral construct expressing the Nt domain of ATG16L1 (residues 1-299; positions 1-897 in ATG16L1 mRNA, not overlapping with the target sequence of the 1025 CRISPR/Cas9 guide). Cells were lysed for Western-blotting with the indicated antibodies. The nomenclature of cells used in subsequent assays is shown below the Western-blot panels (ATG16L1 expression). **b**, Evaluation of the autophagic flux in THP1 cells expressing endogenous ATG16L1 (FL) or ectopic Nt domain (Nt). The indicated cells were treated with bafilomycin A1 (75 nM; 6h) and lysed for Western-blotting with the indicated antibodies. **c**, Endogenous IL-10R expression in engineered THP1 cells. The indicated THP1 strains were incubated with PMA (125 ng/ml; 48 h) or left untreated (as shown), and lysed for Western-blotting with the indicated antibodies. Corrected densitometric quantifications are shown at the bottom of the Western-blot images. **d**, Surface expression levels of IL-10Rs. The indicated cells were incubated with PMA (125 ng/ml; 48 h) and subjected to flow cytometry with irrelevant (Ig) or specific anti-IL-10RA and -IL-10RB antibodies (as indicated). Shown are the average means of fluorescence (MF) from quintuplicate or sextuplicate experimental points \pm s.d. ($n=5$ or $n=6$) for IL-10RA or IL-10RB respectively; n.s. P -value $>0,05$, two-sided Student's t -test). A scheme of the gating and quantification strategy is provided in Supplementary Figure 17. Source data are provided as a Source Data file.



Supplementary Figure 16. Characterization of BMDMs isolated from wild-type and E230 mice. **a**, Expression of the differentiation markers CD11 and F4/80. Bone marrow cells isolated from the indicated mice (FL: wild-type; Nt: E230) were differentiated in vitro (M-CSF 20 ng/ml; 6 days) and subjected to flow cytometry with specific anti-CD11b (left panel) and anti-F4/80 (right panel) antibodies. Shown are the average percentage of positive cells with respect to a control antibody (left axis, white bars, solid dots) and the average mean of fluorescence of the positive cells (MF, right axis, grey bars, white dots) from triplicate experimental points \pm s.d. ($n=3$; n.s.: P -value $>0,05$, two-sided Student's t -test). A scheme of the gating and quantification strategy is provided in Supplementary Figure 17. **b**, Expression levels of ATG16L1 in wild-type and E230 BMDMs. BMDMs were obtained as in **a** from 2 wild-type (FL) and 2 E230 (Nt) mice (as indicated). Cells were lysed for Western-blotting against the shown molecules. **c**, Statistical analysis of nuclear P-STAT3 densitometric signals induced by IL-10, as shown in Fig. 6c. Crude densitometric values were internally normalized as the percentage of the highest value per series. Numbers for P-STAT3 were then normalized against those obtained for total STAT3 (left graph) or H3 (right graph), and the data corresponding to the 5 and 15 min time points were pooled together and evaluated for statistical significance. Shown are mean values \pm s.d. ($n=6$; (*): P -value $<0,05$, two-sided Student's t -test). Source data are provided as a Source Data file.



Supplementary Figure 17. Gating schemes of flow cytometry analyses shown in Supplementary Figures 5d, 15d and 16a. Cells were in all cases gated at the FS/SS plot to select live cells and remove debris. **a, Scheme for Supplementary Figure 5d.** MEFs not expressing or expressing IL-10Rs were stained with IL-10R-specific antibodies. Cells lacking IL-10Rs were used as a negative control to define a threshold leaving approximately 5% of positive cells. Supplementary Figure 5d shows the % and mean of fluorescence (MF) of the cells expressing IL-10Rs that show fluorescence intensity levels above the established threshold. **b, Scheme for Supplementary Figure 15d.** THP1 cells were stained with a control Ig-Alexa-647 or specific anti-IL-10Rs-Alexa-647 antibodies. Supplementary Figure 15d shows crude values of fluorescence intensity (MF) obtained in both conditions. **c, Scheme for Supplementary Figure 16a.** Differentiated BMDMs were stained with irrelevant Ig-BB515 or Ig-Alexa-647 control antibodies, and with specific anti-CD11b-BB515 or anti-F4/80-Alexa-647 antibodies, respectively. The irrelevant controls were used to define thresholds leaving approximately 5% of positive cells. Supplementary Figure 16a shows the % and mean of fluorescence (MF) of the cells stained with anti-CD11b or anti-F4/80 that show fluorescence intensity levels above the established threshold.

SUPPLEMENTARY TABLES 1 TO 5

Supplementary Table 1. Oligonucleotides for PCR

IL-2Rg-Hind3-Kozak-fw	5' gggcccaagcttgccaccatgtgaagccatcattaccattcacatcc 3'
IL-2Rg-Bsph1-rev	5' cccgggtcatgacggtttcaggcttaggggttaacatgg 3'
IL-10RB-Hind3-Kozak-fw	5' gggcccaagcttgccaccatggcgtggagccttgggagctggctggg 3'
IL-10RB-Bsph1-rev	5' cccgggtcatgacgcttggggccctgccaggcggggtc 3'
IL-4RA-EcoR1-Kozak-fw	5' gggcccgaattcgccaccatgggggtgcttggctctgggctcctgttc 3'
IL-4RA-Bsph1-rev	5' cccgggtcatgacagagaccctcatgtatgtgggtccac 3'
IL-6RB-Hind3-Kozak-fw	5' gggcccaagcttgccaccatgtgacgttcagacttggttagtgc 3'
IL-6RB-Bsph1-rev	5' cccgggtcatgacctgaggcatgtagcccttgccttac 3'
IL-12RB2-Hind3-Kozak-fw	5' gggcccaagcttgccaccatggcacatactttagaggatgctcattg 3'
IL-12RB2-Bsph1-rev	5' cccgggtcatgacgagcatgaggagtcacacctcatcttaac 3'
IL-20RA-Hind3-Kozak-fw	5' gggcccaagcttgccaccatgcgggctcccggcggccggccctgc 3'
IL-20RA-Bsph1-rev	5' cccgggtcatgacgttttccatctgcacataaacccc 3'
IL-21R-EcoR1-Kozak-fw	5' gggcccgaattcgccaccatgcgcgtggctgggcccggcccttgc 3'
IL-21R-Bsph1-rev	5' cccgggtcatgacgctggcctgggtccagggtcgaag 3'
IL18R-EcoR1-Kozak-fw	5' gggcccgaattcgccaccatgaattgtagagaattacccttgacc 3'
IL18R-Bsph1-Stop-Not1-rev	5' cccggggcggcgcttagctcatgacagactcggaaagaacaggcaagactccgg 3'
IL18RAP-Hind3-Kozak-fw	5' gggcccaagcttgccaccatgctctgttgggctggatattcttggc 3
IL18RAP-Bsph1-Stop-Not1-rev	5' cccggggcggcgcttagctcatgaccattccttaggctgggagctctccc 3
IL-31RA-Hind3-Kozak-fw	5' gggcccaagcttgccaccatgaagctctctcccagccttcatgtgtaacctg 3'
IL-31RA-Bsph1-Stop-Not1-rev	5' cccggggcggcgcttagctcatgacgacttctccttgggtgctctggaag 3'
IL-33R-Hind3-Kozak-fw	5' gggcccaagcttgccaccatggggttttgatcttagcaattctcac 3'
IL-33R-Bsph1-rev	5' cccgggtcatgacttgctctgggagcgaaggaggagcaaac 3'
IL-17RD-Pci1-fw	5' gggcccacatgtctctggcaggagtgggccagccagcag 3'
IL-17RD-Bsph1-Stop-Not1-rev	5' cccggggcggcgcttagctcatgaccaaagggcgaccgctggagttcatcag 3'

Sequences of the oligonucleotides used to generate DNA constructs expressing tagged IL-Rs by PCR

Supplementary Table 2. Oligonucleotides for site-directed mutagenesis

IL-10RB-F292,L295A-TOP	5' gtcggatgagaatgatgttgctgacaaggcaagtgtcattgcagaagac 3'
IL-10RB-F292,L295A-BOTTOM	5' gtcttctgaatgacacttccttgcagcaacatcattctcatccgac 3'
IL-10RB-F280,F281,F283A-(5M)-TOP	5' ctcatcataacacacttctggctgcctccgtccattgtcggatgagaatgatg 3'
IL-10RB-F280,F281,F283A-(5M)-BOTTOM	5' catcattctcatccgacaatggagcggaggcagccagaagtgtgttatgatgag 3'
IL-2Rg-F307,W310A-TOP	5' gttactgaataaccacgggaacgcttcggcccgagtggtgtgctaaaggac 3'
IL-2Rg-F307,W310A-BOTTOM	5' gtccttagacacaccactggcggccgaagcgttcccgtggtattcagtaac 3'
IL-2Rg-L296,L299,Y303A-(5M)-TOP	5' cgaattcccaccctgaagaacgagaggatgctgttactgaagcccacgggaacgcttcggccgcc 3'
IL-2Rg-L296,L299,Y303A-(5M)-BOTTOM	5' ggcggccgaagcgttcccgtgggcttcagtaacagcatcctctcggttcttcagggtgggaattcg 3'
IL-2Rg-L293,L296,L299,Y303A-(6M)-TOP	5' gacgatccccgaattcccaccgcaagaacgagaggatgctgttactgaagcccacgggaacgcttcggccgcc 3'
IL-2Rg-L293,L296,L299,Y303A-(6M)-BOTTOM	5' ggcggccgaagcgttcccgtgggcttcagtaacagcatcctctcggttcttcagggtgggaattcg 3'
IL-18R1 intron deletion-TOP	5' caacagcacatcattgtataagaactgtaaaaagctactactgg 3'
IL-18R1 intron deletion-BOTTOM	5' ccagtagtagctttttacagtcttatacaatgatgtgctgttg 3'

Sequences of the oligonucleotides used to generate new DNA constructs by site-directed mutagenesis

Supplementary Table 3. Oligonucleotides including the STAT3 operon

STAT3op-Hpa1-Xho1-TOP	5' aacctcgagtgcttcccgaacgttgcttcccgaacgttgcttcccgaacgttgcttcccgaacgt 3'
STAT3op-Hpa1-Xho1-BOTT	5' tcgaacgttcgggaagcaacgttcgggaagcaacgttcgggaagcaacgttcgggaagcactcgagggtt 3'

Sequences of the oligonucleotides used to multimerize the STAT3 enhancer to generate a retroviral STAT3-luciferase reporter system

Supplementary Table 4. Oligonucleotides for CRISPR/Cas9 guides

human ATG16 (78-97)-TOP	5' caccggctgcagagacaggcgttcg 3'
human ATG16 (78-97)-BOTTOM	5' aaaccgaacgcctgtctctgcagcc 3'
human ATG16L1 (1025-1044)-TOP	5' caccgtggaccgcagggttaagctt 3'
human ATG16L1 (1025-1044)-BOTTOM	5' aaacaagcttaaccctgcgggtccac 3'
Mouse Rubicon (29-48)-TOP	5' caccgagtttgtaaagacattcgg 3'
Mouse Rubicon (29-48)-BOTTOM	5' aaaccgaatgtctttcacaaactc 3'

Sequences of the oligonucleotides used to generate CRISPR/Cas9 sgRNAs to reduce the expression of ATG16L1 and Rubicon

Supplementary Table 5. Oligonucleotides for quantitative PCR

Human TNFa-fw	5' cctctctaatcagccctctg 3'
Human TNFa-rev	5' gaggacctgggagtagatgag 3'
Human IL-6-fw	5' actcacctctcagaacgaattg 3'
Human IL-6-rev	5' ccatcttgaaggtcaggttg 3'
Human bActin-fw	5' catgtacgttgctatccaggc 3'
Human bActin-rev	5' ctcttaatgtcacgcacgat 3'
Human GAPDH-fw	5' ggagcgagatccctccaaat 3'
Human GAPDH-rev	5' ggctgtgtcacttctcatgg 3'
Mouse Bcl3-fw	5' ccggaggcccttactacca 3'
Mouse Bcl3-rev	5' ggagtaggggtgagtaggcag 3'
Mouse TNFa-fw	5' ccctcacactcagatcatcttct 3'
Mouse TNFa-rev	5' gctacgacgtgggctacag 3'
Mouse bActin-fw	5' ggctgtattcccctcatcg 3'
Mouse bActin-rev	5' ccagttggaacaatgccatg 3'
Mouse GAPDH-fw	5' aggtcgggtgtaacggattg 3'
Mouse GAPDH-rev	5' ttagaccatgtagtgaggtca 3'

Sequences of the oligonucleotides used to measure mRNA levels by qPCR